NANO LETTERS

2008
Vol. 8, No. 2
398−404

Multisegment Nanowire Sensors for the Detection of DNA Molecules

Xu Wang[†] and Cengiz S. Ozkan*[,‡]

Department of Chemical and Environmental Engineering and Department of Mechanical Engineering, University of California, Riverside, California 92521

Received May 18, 2007; Revised Manuscript Received December 17, 2007

ABSTRACT

We describe a novel application for detecting specific single strand DNA sequences using multisegment nanowires via a straightforward surface functionalization method. Nanowires comprising CdTe–Au–CdTe segments are fabricated using electrochemical deposition, and electrical characterization indicates a p-type behavior for the multisegment nanostructures, in a back-to-back Schottky diode configuration. Such nanostructures modified with thiol-terminated probe DNA fragments could function as high fidelity sensors for biomolecules at very low concentration. The gold segment is utilized for functionalization and binding of single strand DNA (ssDNA) fragments while the CdTe segments at both ends serve to modulate the equilibrium Fermi level of the heterojunction device upon hybridization of the complementary DNA fragments (cDNA) to the ssDNA over the Au segment. Employing such multisegment nanowires could lead to the fabrication more sophisticated and high multispecificity biosensors via selective functionalization of individual segments for biowarfare sensing and medical diagnostics applications.

Nanowire-based field-effect transistors (FET) have been widely used for detection of a variety of biological and chemical species, detection of PH value, detection of metal ions, viruses, proteins, etc.[1−4] In most of these applications, the mechanism of sensing is based on the functionalization of a homogeneous semiconducting nanowire, such as silicon[4] and In_2O_3 nanowires.[5] There is a growing interest in fabricating heterojunction nanowires, which show great potential for applications in nanoelectronics,[6] energy conversion,[7] self-assembly,[8] and controlled positioning of nanowire arrays.[9] Generally, there are two basic morphologies in nanowire heterostructures: radial heterostructures, such as core−shell nanowires, and axial heterostructures, comprising multisegment nanowires. Core−shell nanowires have been used to fabricate coaxially gated nanowire transistors.[10,11] Multisegment nanowires comprise several different material compositions or phases along its length, and their synthesis have been demonstrated in a variety of configurations including the growth of nanowire superlattices via alternating laser ablation of different solid targets. The superlattices inside the nanowires make them engineered materials having a high thermoelectric coefficient,[12] possible uses in p−n junction diodes,[13] and with notable optical properties via photoluminescence characterization.[14]

Electrochemical template synthesis is a versatile technique for producing multisegment nanowires, in which individual segments could be metallic, oxide, binary, or ternary alloys and semiconducting and conducting polymers. And specific functionality including optical, magnetic, or electrical properties could be introduced. Multisegment metallic nanowires synthesized by electrochemistry have been assembled end-to-end by using different linkages, such as biomolecules[15−18] and polymers.[19] Nanowires capped with magnetic metal ends have been aligned between magnetic electrodes.[20] Another application of multisegment nanowires is based on a form of nanowire lithography,[18] with which nanogaps down to 5

Scheme 1. Schematic Diagram of Template Growth of CdTe−Au−CdTe Striped Nanowires[a]

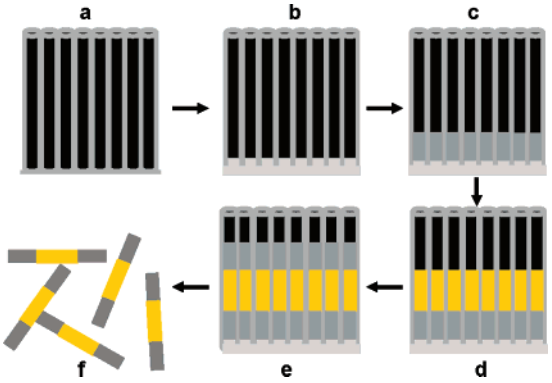

[a] (a) Porous AAO template is used for the deposition. (b) A thin layer of silver is evaporated on one side of AAO, and then approximately 1 μm of silver is filled into the template. (c) CdTe segment is deposited, (d) followed by Au segment, and (e) another CdTe segment. (f) After the silver backside layer and AAO template are dissolved, free CdTe−Au−CdTe nanowires are suspended in the solution.

* To whom correspondence should be addressed. E-mail: cozkan@engr.ucr.edu.
[†] Department of Chemical and Environmental Engineering.
[‡] Department of Mechanical Engineering.

10.1021/nl071180e CCC: $40.75
Published on Web 01/23/2008

Scheme 2. Schematic Illustration of Applying CdTe−Au−CdTe Striped Nanowires for Sensing Specific Biomolecules[a]

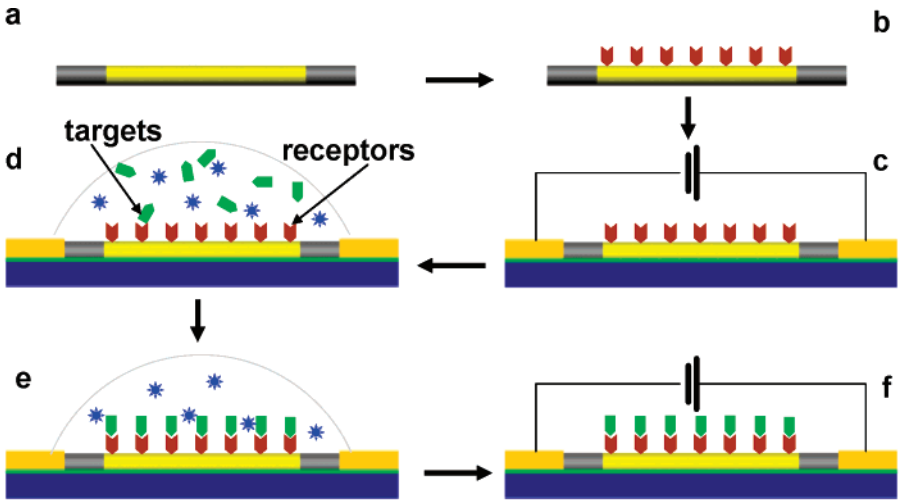

[a] (a) An individual CdTe−Au−CdTe multisegment nanowire, which is fabricated by electrochemistry. (b) Surface functionalization on the Au segment with thiol-terminated molecules. (c) Fabricated modified nanowire FET device using lithography. (d) Immerse the nanowire into the solution containing different biospecies. (e) Specific biomolecules (targets) are self-assemblied to the receptors at the nanowire surface. (f) Sensitive conductance responses from the device are reflected by $I-V$ curves after bound with targets.

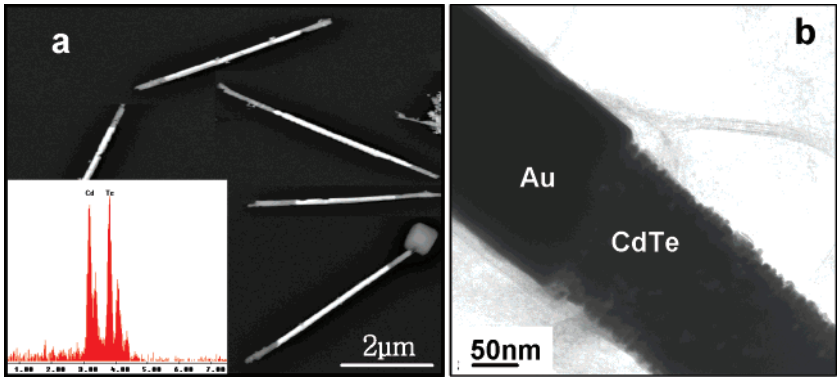

Figure 1. (a) Scanning electronic microscopy (SEM) image of CdTe−Au−CdTe heterostructures. Inset: EDS spectrum of CdTe segments. (b) Transmission electron micrography (TEM) image of the interconnection between CdTe and Au segments, demonstrating the nonuniform deposition of the electrochemistry.

nm could be created.[21,22] Composite nanowires with semiconductor layers sandwiched between metal segments have also been reported, and their photoelectrical effects in such metal-semiconductor nanowire heterostructures have been studied.[23]

To our knowledge, only a few studies on other potential applications of metal-semiconductor heterostructures have been reported. For the first time, we report the sensing capability of multisegment nanowires for ssDNA fragments in this paper. Multisegment or striped nanowires comprising CdTe−Au−CdTe sequences have been synthesized via traditional electrochemistry using porous anodic alumina oxide (AAO) templates as "molds". CdTe has become one of the most attractive semiconductors because of its optimum energy band gap (E_g = 1.44 eV) and high absorption coefficient due to its direct band gap.[24] The Au segment is sandwiched between two CdTe segments because of its active surface functionalization capability. Thiolates anchored onto gold substrates via chemisorption have been investigated for many years, and it turns out that the thiol groups form specially and strongly bonds to the gold surface.[25] In our experiments, free individual striped nanowires are fixed across Au contacts using electron beam lithography. ssDNA fragments with a thiol functional group at one end are bound to the Au segment of the nanowires and serve as the receptor groups. The modulation of nanowire conductance before and after binding and hybridization of specific DNA target molecules have been accessed using back-gated current−voltage measurements. This sensor configuration is much more sensitive compared to the case of individual metallic nanowires in monitoring conductivity change, since much smaller modulations in electrical signals can be realized using the field effect transistor configuration which serves as an inherent amplifier where the Fermi level is modulated across the semiconductor segments. Furthermore, this configuration is much more capable compared to the case of a single semiconducting nanowire sensor since the metallic segment provides a great functionality in selectively binding probe molecules for sensing.

CdTe−Au−CdTe heterojunction nanowires were fabricated using electrochemical deposition in anodic alumina oxide (AAO) templates with 200 nm diameter pores (An-

odizc, Whatman) by altering electrolyte solutions (Scheme 1). The deposition process followed the method described by Pena et al.[23] Briefly, a silver film was coated on one side of a AAO template by thermal evaporation. The AAO was then attached to a stripe of conductive copper tape with the uncoated side facing up. The set served as the working electrode in a standard three-electrode electrochemical cell. Before depositing CdTe, Ag was deposited galvanostatically using a commercially available electrolyte (Techni silver cyless II) at 1 mA/cm^2 for 5 min. CdTe segments of the nanowire were deposited at 10 mA/cm^2 for 15 min from the electrolyte at room temperature. Au segments were deposited from a commercial solution (Techni Gold 25 ES) at 2 mA/cm^2 for 15 min. Finally, another segment of CdTe was deposited for 15 min. CdTe plating solutions were prepared by mixing 0.3 M $CdSO_4$, 0.006 M TeO_2, and 0.5 M H_2SO_4 at room temperature. The deposition conditions of each segment were exploited using a Hull Cell experiment in advance. After the completion of deposition, the AAO template was gently detached from copper tape by rinsing with acetone, and the silver backing and silver segment inside the pores were removed by dipping the template within 70 vol % nitric acid solution. The template was dissolved in a 6 M NaOH solution. Eventually, the free nanowires were washed repeatedly using deionized water.

The surface modification of the nanowires was accomplished by adding biomolecules with a thiol functional group. A single strand of DNA(I) with the sequence of GCCCTTCAGTCGCCTATCCACCAT[3THS](Sigma Genosys) was used in the experiments. CdTe−Au−CdTe nanowires were first immersed in ethanol for 20 min, and then they were incubated overnight at room temperature in the ssDNA(I) solution at pH = 7. During the incubation process, the ssDNA(I) molecules were bound to the Au segment surfaces via thiol linkage. After the CdTe−Au−CdTe nanowires were cleaned by rinsing with deionized water several times, biosensors based on the configuration of nanowire field effect transistors (FET) were fabricated using electron beam lithography. The CdTe−Au−CdTe FET devices were immersed into different solutions for sensing: a buffer solution (pH = 7.2) without DNA, a 500 μM ssDNA(II) solution, and a 500 μM ssDNA(III) solution. Complementary ssDNA(II) fragments with the sequence ATGGTGGATAGGCGACTCAAGGGC (Sigma Genosys) were hybridized to the ssDNA(I). The buffer solution and mismatched ssDNA(III) fragments with the sequence of GTGTGTGGAGTTACAAGCCTGAGTC (Sigma Genosys) were used for control experiments. DNA hybridization happened in a water bath at 42 °C for 4 h. Current voltage ($I-V$) measurements were conducted with an Agilent 4155C semiconductor parameter analyzer, and the modulation of the conductance was recorded. Scheme 2 shows the steps involved in fabricating the multisegment nanowire FET devices for detecting specific biological species.

The morphology and heterostructure of CdTe−Au−CdTe nanowires are shown in Figure 1a. Nanowires are mostly 230 nm in diameter and 5 μm in length. Because of the lower energy of the scattered electrons of CdTe than that of Au,

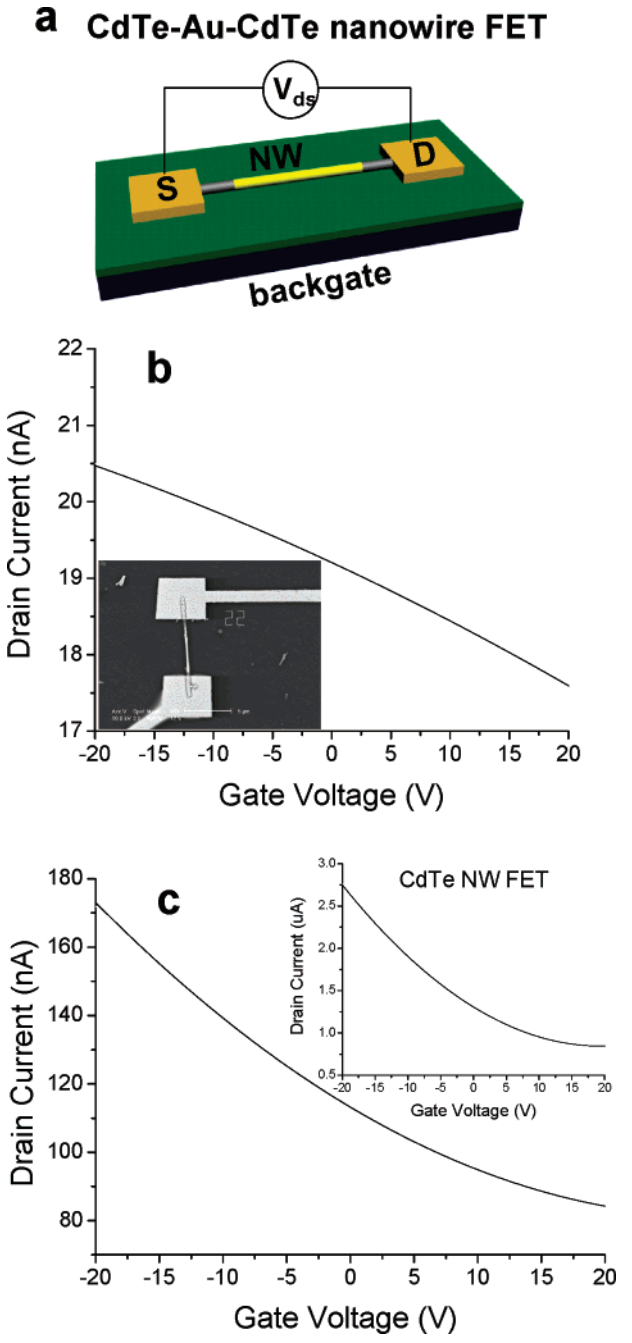

Figure 2. (a) Schematic of CdTe−Au−CdTe nanowire field-effect transistor. A drop of solution containing suspended CdTe−Au−CdTe nanowires was deposited onto a P^+ silicon chip capped SiO_2. The P^+ silicon layer acted as the back-gate in the field effect transistor configuration. E-beam lithography was utilized to deposit the metal electrodes on each end of individual CdTe−Au−CdTe nanowire. (b) Transfer charateristics: $I_d(V_{gs})$ at V_{ds} = 1 V of CdTe−Au−CdTe FET with a gate oxide thickness of 500 nm. Inset is the SEM image of CdTe−Au−CdTe nanowire FET. (c) $I-V_g$ at V_{ds} = 1 V of CdTe−Au−CdTe FET with a gate oxide thickness of 50 nm. Because gate effect in FET is related to the thickness of gate dielectric, the performance of CdTe−Au−CdTe nanowire FET is more discernible when Si substrate is capped with thinner SiO_2. $I-V_g$ measurement (V_{ds} = 1 V) of CdTe nanowire FET device (inset).

CdTe segments appear darker in the images. The chemical compositions of CdTe segments are analyzed using X-ray energy-dispersive spectroscopy (Figure 1a, inset). The spec-

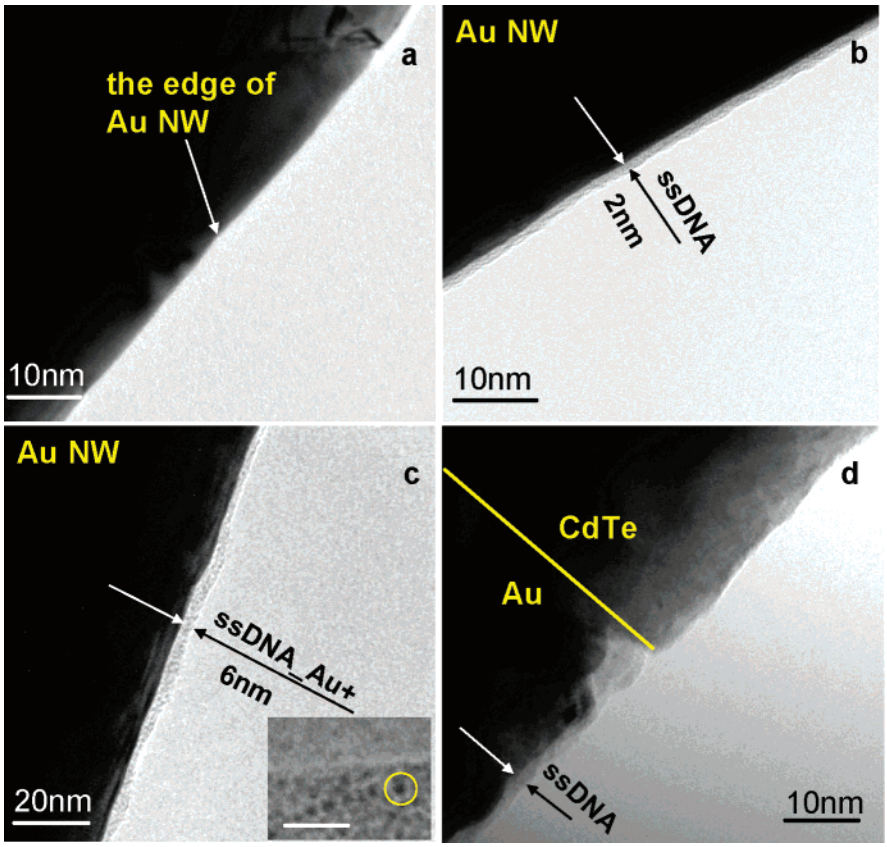

Figure 3. Surface functionalization of CdTe−Au−CdTe composite nanowire. (a) Clear edge of gold nanowire is observed. The black is Au nanowire body, and the white is the background. (b) Thiol-terminated ssDNA molecules bound to the gold surface, forming a thin layer less than 2 nm. (c) Gold nanoparticles are adsorbed around the Au surface due to the electrostatic force between positive charges of gold nanoparticles and negative charges of ssDNA molecules. Inset: High magnification TEM image of ssDNA layer with Au nanoparticles adsorbed. One nanoparticle is circled. The scale bar is 10 nm. (d) The interface area between the Au and CdTe segment after thiol-terminated ssDNA funcationalization. Au is surrounded by an ssDNA thin layer, while the surface of CdTe remains unchanged.

trum indicates the sample is composed of Cd and Te elements, and the atomic ratio of Cd and Te is about 1:1. A transmission electron micrograph in Figure 1b shows the connectivity of CdTe and Au segments. The interface between CdTe and Au is not highly uniform. The changing of electrolytes during the nanowire growth process results in the diffusion of ions in the previous segment.[16] The interface of the composite nanowires plays a considerable role in the electromagnetic interaction between segments under some dimensions.[26] Therefore, the effect of interfaces between CdTe and Au segments on the nanowire's electrical properties has been exploited. Transport measurements are conducted on the FETs made of CdTe−Au−CdTe nanowires by sweeping the gate voltage (V_g) at a constant source−drain voltage (V_{ds}). The three terminal configuration (source−drain−gate) is shown in Figure 2a. Figure 2b displays the $I-V_g$ curve of a CdTe−Au−CdTe device. As the current decreases with increasing gate voltage, the CdTe−Au−CdTe nanowire demonstrates a p-type semiconductor behavior. $I-V_g$ measurements of several other CdTe−Au−CdTe nanowires indicated similar behavior (Figure 2c). In a control experiment, electrical characterizations of bare CdTe nanowires, which were synthesized using the same electrochemical conditions, are performed. By comparison, uniform CdTe nanowires indicate higher electrical conductance (Figure 2c inset). The Au−CdTe junction of the heterojunction nanowires is the fundamental reason for this variation of the conductance. $I-V_g$ data of homogeneous CdTe nanowires also exhibit similar p-FET behavior (Figure 2c inset). From this comparison, we can conclude that the CdTe−Au interfaces of the heterojunction nanowires do not result in a significant degradation of its electrical properties or $I-V$ characteristics when the Fermi level is modulated by the applied gate voltage.

Inorganic 1-D nanostructures can be employed in highly selective biosensing via chemical modification of the surface. Different ligands prefer to adsorb to different surfaces.[27] For example, the isocyanides selectively bind to platinum surfaces,[28] and the carboxylic acids selectively bind to metal oxides surfaces.[29] Thiols have a high affinity for Au surfaces and form self-assembled monolayers.[25] Specific binding of thiol-terminated ssDNA fragments with the Au segment of CdTe−Au−CdTe nanowires is reflected in the TEM images in Figure 3. A very smooth Au surface and sharp edge are observed before incubating the nanowires with the ssDNA solution (Figure 3a). After the chemisorption of the thiols at the end of the ssDNA fragments, a very thin film nearly 2 nm thick is wrapped around the Au surface (Figure 3b). The thin film being composed of the ssDNA fragments is demonstrated by immersing the nanowires into a solution containing positively charged Au nanoparticles (1 nm diameter) for 2 h. The sample is then gently rinsed with

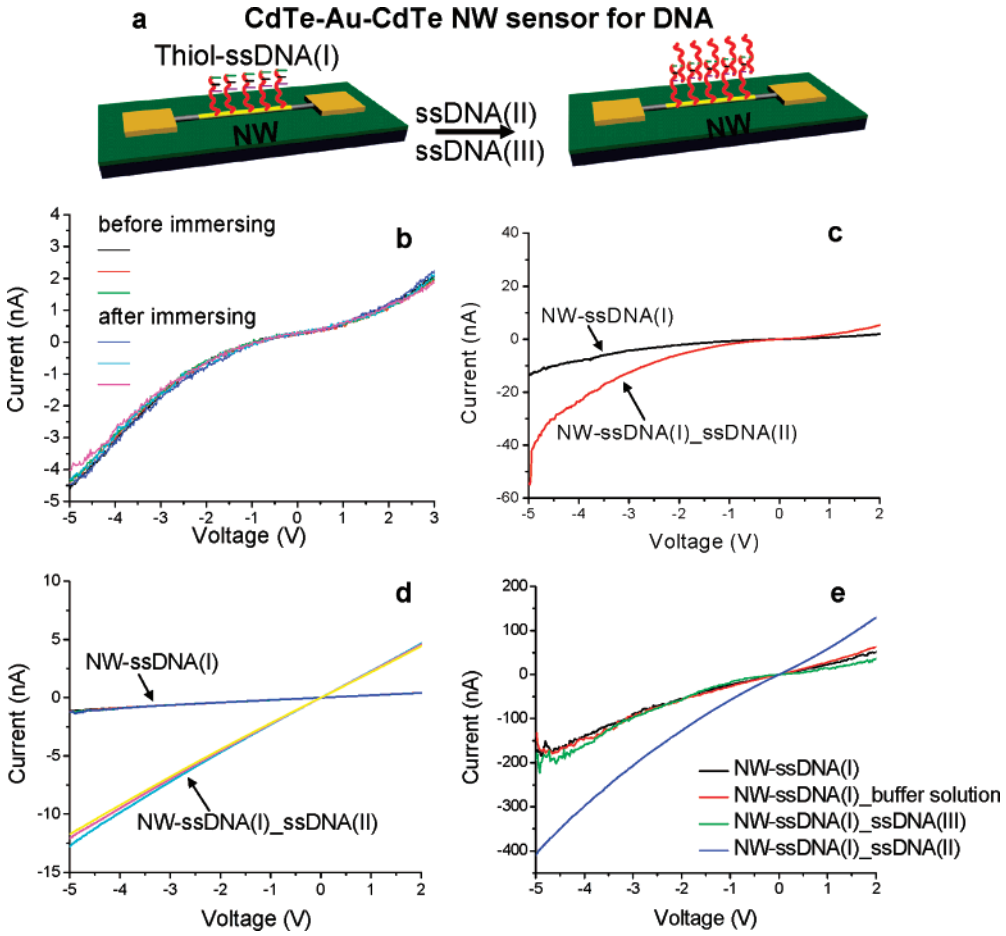

Figure 4. (a) Schematic illustration of surface receptors modified CdTe−Au−CdTe nanowire FET for the detection of DNA. Thiol-terminated ssDNA(I) binding to the Au segment serves as the surface receptors. (b) *I*−*V* responds from a CdTe−Au−CdTe nanowire sensor before immersion in water and after immersion in water at 42 °C. No changes in conductance happen. (c) Conductance responds from the CdTe−Au−CdTe nanowire device for ssDNA(II), which is matched with the receptor ssDNA(I). (d) Conductance responds for ssDNA(II) from another CdTe−Au−CdTe nanowire device. (e) Different sensing responses for the solution without DNA molecules, mismatched ssDNA(III), and matched ssDNA(II) are presented by the *I*−*V* curves measured from a CdTe−Au−CdTe device.

deionized water and is subsequently prepared for TEM imaging (Figure 3c). The film around the Au surface turns darker and thicker (6 nm). Gold nanoparticles are responsible for this increase of the thickness and the change in image contrast. Due to the negative charge associated with the backbone of the ssDNA molecules, positively charged Au nanoparticles are electrostatically absorbed. Comparatively, the surface of a CdTe segment undergoes no change during the process of surface functionalization, which is elucidated by the TEM image comparing the CdTe and Au segments (Figure 3d). ssDNA specifically binds to the Au segment of the nanowire and does not alter the CdTe segment. Although thiols can be capped on CdTe nanoparticles,[30,31] such a synthesis is finished via a hydrothermal route, where the thiolates are utilized as size-regulating and stabilizing agents. Under the experimental conditions described in this paper, thiolates do not form bonds to the surface of CdTe segments; the thiol groups present at the end of ssDNA(I) fragments anchor only onto the surface of the Au segment.

Modified CdTe−Au−CdTe multisegment nanowires are assembled into FET devices using lithographic procedures (Figure 4a). Au contacts at nanowire ends are patterned via electron beam lithography and electron beam evaporation. The nanowire contacts are tested by immersing the FET devices into a water bath at 42 °C for several hours. Repeated *I*−*V* measurements (Figure 4b) demonstrate that the nanowire contacts are stable and reliable so that the effect of water bath on the device can be excluded. An increase in conductance recorded from a CdTe−Au−CdTe nanowire device is observed only after adding a complementary ssDNA(II) solution (Figure 4c). A similar increase in conductance is observed in other nanowire devices as well (Figure 4d). The increase in conductance is due to an increase in the number of negative charges at the device surface associated with binding of negatively charged ssDNA(II). In the sensor configuration, ssDNA(I) serves not only as receptors for the target molecules but also as a gate dielectric for modulating the Fermi level. When ssDNA(II) is added, it hybridizes with ssDNA(I) instead of binding to the metal surface directly. Even though ssDNA(II) fragments are dried after the device is taken out of the solution for electrical measurements, the DNA fragments are still negatively charged because they were initially dissolved in a buffer solution resulting in the adsorption of ions. Electronic transport in dry single-stranded and double-stranded DNA fragments has been explored extensively by many researchers

in the field. It has been noted extensively that, after most of the drying processes, residual water molecules stay adhered to the DNA structure, along with cations counterbalancing the backbone negative charges of DNA fragments.[32−35] Water molecules are easily adsorbed on the hydrophilic phosphoric acid chains by forming hydrogen bonds.[36,37] Hydrophilic phosphoric acid chains control the number of water molecules adsorbed on the DNA fragments, as suggested by Otsuka et al.[36] and Ha et al.[37] Also, the effect of environment on the DNA fragments after drying cannot be ignored.[38,39] Under high humidity levels, water molecules will further accumulate on the phosphate backbone of DNA fragments.[39] Electrical measurements in this paper are conducted in a laboratory facility with daily average humidity levels between 30% and 45%. Therefore, ssDNA(II) fragments bear negative charges with water molecules surrounding them. The binding of charged DNA is analogous to exerting a negative gate voltage on the device. Thus, the conductivity of the p-type CdTe−Au−CdTe nanowire increases when complementary ssDNA(II) fragments hybridize to the receptor ssDNA(I) fragments. Although changes in conductivity could happen when sensing species that could bind nonspecifically,[40] a remedy is to apply subsequent washing steps to reduce and eliminate the possibility of nonspecific sensing. No covalent linkage between ssDNA fragments and a bare metal electrode can form; hence any ssDNA fragments that are nonspecifically adsorbed can be rinsed off after the hybridization step. To further verify the nature of the observed conductivity change, control experiments have been carried out as well. A CdTe−Au−CdTe nanowire sensor is first used to detect a pure buffer solution and a ssDNA(III) solution. No substantial changes in conductance are observed after adding these two solutions (Figure 4e, red and green curves). The very small variations in conductivity from the ssDNA(III) sample (Figure 4e, green curve) could be the result of nonspecific interactions of negatively charged ssDNA(III) fragments with the nanowire sensor. The same device is then prepared for detecting ssDNA(II). An apparent increase in conductivity is shown in Figure 4e (blue curve), which presents a trend similar to those of the other two devices (Figure 4c and d). This clearly demonstrates the selective sensing capability of the CdTe−Au−CdTe nanowire sensors.

The sensitivity of the device has been studied by sensing ssDNA(II) at lower concentrations (Figure 5). ssDNA(II) solution was diluted to 1 nM, 1 μM, and 10 μM solutions. $I-V$ measurements recorded from a modified CdTe−Au−CdTe nanowire are shown with the blue curve in Figure 5. When the device was exposed to a 1 nM ssDNA(II) solution, the $I-V$ curve remained unchanged (green). After immersing in a 1 μM ssDNA(II) solution, an increase in conductivity was observed (red). Conductivity increased further with a higher concentration solution ($I-V$ results shown for 10 μM ssDNA (II) with the black curve). The more ssDNA(II) fragments are added, then the more negative charges are accumulated on the nanowire surface. As a result, a larger negative gate voltage is exerted on the system, resulting in an increased conductivity

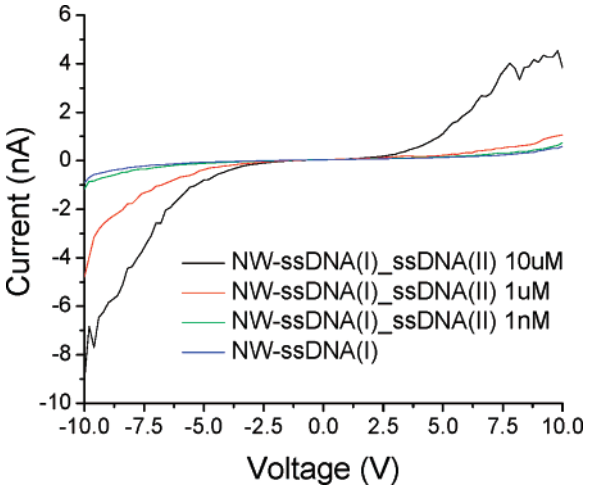

Figure 5. CdTe−Au−CdTe nanowire sensor detecting ssDNA-(II) at different low concentrations. Electrical measurements are made before detecting (blue curve), after detecting 1 nM ssDNA-(II) (green curve), 1 μM (red curve), and 10 μM (black curve).

for the p-type nanowires. Overall, we successfully monitored the sensing capability of the CdTe−Au−CdTe nanowires down to the 1 μM concentration. The interface of CdTe and Au segments in the nanowire could pause a limitation for sensitivity; changing of electrolytes during nanowire synthesis could result in the formation of nonuniform interfaces and defects. Future optimization of electrochemical deposition to obtain sharper interfaces in the composite nanowires as well as employing smaller diameter nanowires will improve the sensor detection capabilities toward much lower target molecule concentrations.

In summary, multisegment CdTe−Au−CdTe nanowires have been synthesized using electrochemical deposition into porous alumina templates which indicated a p-type behavior. After functionalized by thiol-ended ssDNA receptors, the nanowires are used to fabricate sensors with a field-effect transistor (FET) configuration, which could be used for ultrasensitive detection of biomolecules based on the modulation of nanowire conductance. Adding ssDNA(II) molecules, which hybridizes with the receptor molecules at the nanowire surface, results in significant modulation of conductance. This process is analogous to applying a negative bias voltage on the backgate of a CdTe−Au−CdTe FET. Our results illustrate the promise of multisegment heterojunction nanowire sensors based on selective segment functionalization for ultrasensitive detection of a broad range of biological and chemical species. Possible applications for the future include multiplexed multisegment nanowire sensors for simultaneous detection of multiple species. Other possibilities for different kinds of multisegment nanowires may include selectively employing the optical and magnetic properties in addition to the electrical properties of individual segments for multifunctional sensing.

Acknowledgment. This work was supported by the Center for Nanoscience Innovation for Defense (CNID) funded by the Defense MicroElectronics Activity (DMEA),

the Focus Center Research Program on Functional Engineered Nano Architectonics (FENA) funded by the DARPA (Defense Advanced Research Projects Agency) and the Semiconductor Research Corporation (SRC), and the Center for Nanotechnology for Treatment, Understanding, and Monitoring of Cancer (NANO-TUMOR) funded by the National Cancer Institute (NCI).

References

(1) Cui, Y.; Wei, Q. Q.; Park, H. K.; Lieber, C. M. *Science* **2001**, *293*, 1289−1292.
(2) Zheng, G. F.; Patolsky, F.; Cui, Y.; Wang, W. U.; Lieber, C. M. *Nat. Biotechnol.* **2005**, *23*, 1294−1301.
(3) Hahm, J.; Lieber, C. M. *Nano Lett.* **2004**, *4*, 51−54.
(4) Patolsky, F.; Zheng, G. F.; Lieber, C. M. *Anal. Chem.* **2006**, *78*, 4260−4269.
(5) Li, C.; Curreli, M.; Lin, H.; Lei, B.; Ishikawa, F. N.; Datar, R.; Cote, R. J.; Thompson, M. E.; Zhou, C. W. *J. Am. Chem. Soc.* **2005**, *127*, 12484−12485.
(6) Bjork, M. T.; Ohlsson, B. J.; Thelander, C.; Persson, A. I.; Deppert, K.; Wallenberg, L. R.; Samuelson, L. *Appl. Phys. Lett.* **2002**, *81*, 4458−4460.
(7) Kayes, B. M.; Atwater, H. A.; Lewis, N. S. *J. Appl. Phys.* **2005**, *97*, 114302−114313.
(8) Love, J. C.; Urbach, A. R.; Prentiss, M. G.; Whitesides, G. M. *J. Am. Chem. Soc.* **2003**, *125*, 12696−12697.
(9) Hangarter, C. M.; Myung, N. V. *Chem. Mater.* **2005**, *17*, 1320−1324.
(10) Wu, Y.; Xiang, J.; Yang, C.; Lu, W.; Lieber, C. M. *Nature* **2004**, *430*, 704−704.
(11) Lauhon, L. J.; Gudiksen, M. S.; Wang, C. L.; Lieber, C. M. *Nature* **2002**, *420*, 57−61.
(12) Li, D. Y.; Wu, Y.; Fan, R.; Yang, P. D.; Majumdar, A. *Appl. Phys. Lett.* **2003**, *83*, 3186−3188.
(13) Cheng, G. S.; Kolmakov, A.; Zhang, Y. X.; Moskovits, M.; Munden, R.; Reed, M. A.; Wang, G. M.; Moses, D.; Zhang, J. P. *Appl. Phys. Lett.* **2003**, *83*, 1578−1580.
(14) Panev, N.; Persson, A. I.; Skold, N.; Samuelson, L. *Appl. Phys. Lett.* **2003**, *83*, 2238−2240.
(15) Chen, M.; Guo, L.; Ravi, R.; Searson, P. C. *J. Phys. Chem. B* **2006**, *110*, 211−217.
(16) Bridget Wildt, P. M.; Searson, Peter C. *Langmuir* **2006**, *22*, 10528−10534.
(17) Salem, A. K.; Chen, M.; Hayden, J.; Leong, K. W.; Searson, P. C. *Nano Lett.* **2004**, *4*, 1163−1165.
(18) Awang, A. A.; Lee, J.; Jenikova, G.; Mulchandani, A.; Myung, N. V.; Chen, W. *Nanotechnology* **2006**, *17*, 3375−3379.
(19) Gu, Z. Y.; Chen, Y. M.; Gracias, D. H. *Langmuir* **2004**, *20*, 11308−11311.
(20) Bentley, A. K.; Trethewey, J. S.; Ellis, A. B.; Crone, W. C. *Nano Lett.* **2004**, *4*, 487−490.
(21) Liu, S. H.; Tok, J. B. H.; Bao, Z. N. *Nano Lett.* **2005**, *5*, 1071−1076.
(22) Qin, L. D.; Park, S.; Huang, L.; Mirkin, C. A. *Science* **2005**, *309*, 113−115.
(23) Pena, D. J.; Mbindyo, J. K. N.; Carado, A. J.; Mallouk, T. E.; Keating, C. D.; Razavi, B.; Mayer, T. S. *J. Phys. Chem. B* **2002**, *106*, 7458−7462.
(24) Zhao, A. W.; Meng, G. W.; Zhang, L. D.; Gao, T.; Sun, S. H.; Pang, Y. T. *Appl. Phys. A* **2003**, *76*, 537−539.
(25) Ulman, A. *Chem. Rev.* **1996**, *96*, 1533−1554.
(26) Mock, J. J.; Oldenburg, S. J.; Smith, D. R.; Schultz, D. A.; Schultz, S. *Nano Lett.* **2002**, *2*, 465−469.
(27) Bauer, L. A.; Birenbaum, N. S.; Meyer, G. J. *J. Mater. Chem.* **2004**, *14*, 517−526.
(28) Hickman, J. J.; Laibinis, P. E.; Auerbach, D. I.; Zou, C. F.; Gardner, T. J.; Whitesides, G. M.; Wrighton, M. S. *Langmuir* **1992**, *8*, 357−359.
(29) Laibinis, P. E.; Hickman, J. J.; Wrighton, M. S.; Whitesides, G. M. *Science* **1989**, *245*, 845−847.
(30) Ma, J.; Chen, J. Y.; Guo, J.; Wang, C. C.; Yang, W. L.; Xu L.; Wang, P. N. *Nanotechnology* **2006**, *17*, 2083−2089.
(31) Guo, J.; Yang, W. L.; Wang, C. C. *J. Phys. Chem. B* **2005**, *109*, 17467−17473.
(32) Otto, P.; Clementi, E.; Ladik, J. *J. Chem. Phys.* **1983**, *78*, 4547 -.
(33) Lewis, J. P.; Ordej'on, P.; Sankey, O. F. *Phys. Rev. B* **1997**, *55*, 6880-.
(34) York, D. M.; Lee, T. S.; Yang, W. *Phys. Rev. Lett.* **1998**, *80*, 5011-.
(35) Ye, Y. J.; Jiang, Y. *Int. J. Quantum Chem.* **2000**, *78*, 112−130.
(36) Otsuka, Y.; Lee, H.-Y.; Gu, J.-H.; Lee, J.-O.; Yoo, K.-H.; Tanaka, H.; Tabata, H.; Kawai, T. *Jpn. J. Appl. Phys.* **2002**, *41*, 891.
(37) Ha, D. H.; Nham, H.; Yoo, K.-H.; So, H.-M.; Lee, H.-Y.; Kawai, T. *Chem. Phys. Lett.* **2002**, *355*, 405.
(38) Jo, Y. S.; Lee, Y.; Roh, Y. *J. Korean Phys. Soc.* **2003**, *43*, 909−913.
(39) Kleine-Ostmann, T., Jördens, C.; Baaske, K.; Weimann, T.; Hrabe de Angelis, M.; Koch, M. *Appl. Phys. Lett.* **2006**, *88*, 102102.
(40) Chen, R. J.; Choi, H. C.; Bangsaruntip, S.; Yenilmez, E.; Tang, X. W.; Wang, Q.; Chang, Y. L.; Dai, H. J. *J. Am. Chem. Soc.* **2004**, *126*, 1563−1568.

NL071180E